Published in final edited form as:
Dev Biol. 2011 October 1; 358(1): 137–146. doi:10.1016/j.ydbio.2011.07.017.

BzpF is a CREB-like transcription factor that regulates spore maturation and stability in *Dictyostelium*

Eryong Huang[1], **Shaheynoor Talukder**[2], **Timothy R. Hughes**[2], **Tomaz Curk**[3], **Blaz Zupan**[3], **Gad Shaulsky**[1], and **Mariko Katoh-Kurasawa**[1,*]

[1]Department of Molecular and Human Genetics, Baylor College of Medicine, One Baylor Plaza, Houston TX 77030, USA

[2]Banting and Best Department of Medical Research, University of Toronto, Toronto, ON, M5S 3E1, Canada

[3]Faculty of Computer and Information Science, University of Ljubljana, Trzaska cesta 25, SI-1001 Ljubljana, Slovenia

Abstract

The cAMP response element-binding protein (CREB) is a highly conserved transcription factor that integrates signaling through the cAMP-dependent protein kinase A (PKA) in many eukaryotes. PKA plays a critical role in *Dictyostelium* development but no CREB homologue has been identified in this system. Here we show that *Dictyostelium* utilizes a CREB-like protein, BzpF, to integrate PKA signaling during late development. *bzpF*$^{-}$ mutants produce compromised spores, which are extremely unstable and germination defective. Previously, we have found that BzpF binds the canonical CRE motif in vitro. In this paper, we determined the DNA binding specificity of BzpF using protein binding microarray (PBM) and showed that the motif with the highest specificity is a CRE-like sequence. BzpF is necessary to activate the transcription of at least 15 PKA-regulated, late-developmental target genes whose promoters contain BzpF binding motifs. BzpF is sufficient to activate two of these genes. The comparison of RNA sequencing data between wild type and *bzpF*$^{-}$ mutant revealed that the mutant fails to express 205 genes, many of which encode cellulose-binding and sugar-binding proteins. We propose that BzpF is a CREB-like transcription factor that regulates spore maturation and stability in a PKA-related manner.

Introduction

Cyclic AMP and cAMP-dependent protein kinase A signaling regulate many cellular events in various eukaryotes. In *Dictyostelium discoideum*, intracellular cAMP plays a central role in development (Saran et al., 2002). PKA is required for early developmental events, including cell aggregation and regulation of gene expression, and for later events, including the transition from slug to fruiting body and the terminal differentiation of spores and stalk cells (Loomis, 1998). The molecular mechanisms that follow PKA activation are largely unknown.

*Correspondence should be addressed to: Mariko Katoh-Kurasawa, Department of Molecular and Human Genetics, Baylor College of Medicine, One Baylor Plaza, Houston TX 77030, USA, mkatoh@bcm.edu, TEL: (713) 798-8308, Fax: (713) 798-1021.

The cAMP response element binding protein, CREB, is a basic-leucine zipper (bZIP) transcription factor and a central downstream target of PKA in many eukaryotes. Dimeric CREB proteins bind the conserved DNA sequence 5′ TGACGTCA 3′, CRE, which is found in the promoters of many cAMP-inducible genes (Montminy et al., 1986), regulating the transcription of target genes in response to increased intercellular cAMP (Johannessen et al., 2004). In mammalian cells, PKA phosphorylates Ser133 in the signal-responsive Kinase-Inducible Domain (KID) of CREB (Gonzalez et al., 1991). CREB phosphorylation leads to interaction with the KIX domain of the co-activators CBP and p300. CREB also has two glutamine-rich domains, which attract the basal transcriptional machinery TFIID (Mengus et al., 2005), and a bZIP domain, which mediates dimerization and DNA binding (Dang et al., 1989; O'Shea et al., 1989).

CREB belongs to the large CREB/ATF family. One of the CREB/ATF subfamilies consists of membrane-bound transcription factors. For example, the liver-specific CREB-like protein CREB3L3/CREB-H binds the canonical CRE, as well as CRE-like sequences, such as the box-B element, and it can suppress hepatoma cell proliferation (Chin et al., 2005; Omori et al., 2001). CREB3L1/OASIS also binds CRE and CRE-like sequences and functions in bone formation (Murakami et al., 2009; Omori et al., 2002). Most members of this subfamily localize to the endoplasmic reticulum (ER) and respond to ER stress (Kondo et al., 2005; Zhang et al., 2006).

The pivotal role of PKA activity in development and in the regulation of gene expression suggested that CREB might have a central function in *Dictyostelium* development as well, but numerous attempts to isolate the *Dictyostelium* CREB have failed. In this study, we report that BzpF is a CREB-like transcription factor that functions downstream of PKA during the late stages of *Dictyostelium* development and regulates sporulation. Loss of BzpF results in severe defects in spore maturation and maintenance.

Material and Methods

Cell culture, strain maintenance, and development

We maintained *Dictyostelium discoideum* strains, which are described in Table S1, at 22°C in HL5 liquid medium (Sussman, 1987) with the indicated supplements. We collected cells at the mid-log growth phase and washed them to induce development (Shaulsky and Loomis, 1993). We deposited 5×10^7 cells on a 16 cm^2 nitrocellulose filter placed on top of a paper pad soaked in 2 ml of PDF buffer (20.1 mM KCl, 5.3 mM $MgCl_2$, 9.2 mM K_2HPO_4, 13.2 mM KH_2PO_4, 0.5 mg/ml streptomycin sulfate, pH 6.4) and incubated them at 22°C in a humid chamber in the dark. When the cells were antibiotic-resistant, we grew them without antibiotics for 24 hours before development.

Plasmid construction and mutant generation

bzpF (DDB_G0279529) is a single-copy gene on the Crick strand of chromosome 3, coordinates 2206682 to 2208577. To knock *bzpF* out, we first amplified the flanking regions of the gene by PCR using two primer sets; (1) bZIP14NKOA5-sacII: 5′-TCCCGCGGCCCATTTTGTTCTGAATCTCATT-3′ and bZIP14NKOA3-hindIII: 5′-TCAAGCTTTCTTGTTGGCTACCATTGGA-3′ (2) bZIP14NKOB5-kpnI: 5′-TCGGTACCCTCCAATCCCTTCTCCTCAA-3′ and bZIP14NKOB3-sacII: 5′-TCCCGCGGCACCTCACTTGAACGTCGTC-3′, and ligated the products to each other after *Sac*II digestion. After amplifying the ligated fragment with the outside primer set, we cloned the products into the *Kpn*I and *Hind*III sites of a modified pLPBLP plasmid (Faix et al., 2004) of which the *Sac*II site was removed (pLPBLPΔSacII). The resulting construct is a *bzpF*-knockout vector with a deletion of most of the *bzpF* coding-region (+414 to +1654).

We linearized the plasmid with *Sac*II and transformed it into AX4 cells (Adachi et al., 1994; Kuspa and Loomis, 1992). We selected the transformants with 10 μg/ml Blasticidin and verified that *bzpF* was knocked out by PCR across the homologous recombination junctions and by quantitative RT-PCR.

For *bzpF* overexpression, we cloned the coding region of *bzpF* from +10 to +1885 under the *actin15* promoter in the pDXA-GFP2 vector (Levi et al., 2000), transformed it into *bzpF*$^{-}$ cells and selected for resistance to 10 μg/ml G418.

Protein Binding Microarrays assay

We purified the GST-fused bZIP region of the BzpF protein (BzpFzip-GST) after expression in *E. coli* as described (Parikh et al., 2010a). We used the fusion protein to analyze BzpF binding site specificity using two different Protein Binding Microarray (PBM) designs, with oligonucleotide sequences as described (Berger et al., 2008; Lam et al., 2011) and protocols as described (Berger et al., 2006; Lam et al., 2011). In downstream analyses, we used a relaxed E-score threshold (0.4 instead of 0.45), following (Grove et al., 2009), and because all of the 8-mers between 0.4 and 0.45 contained either the core CREB site (ACGT) and/or a full CREB half-site (TGACG/CGTCA), and the same 8-mers scored highly in both experiments. In genomic scans, we eliminated data of 8-mers that did not meet the significance threshold in any of the experiments. We used the first data set to generate the position weighted matrix for BzpF binding and to calculate the binding scores. The results of both analyses are provided in supplementary dataset S1.

Electrophoresis mobility shift assay

We used the fusion protein BzpFzip-GST in an electrophoresis mobility shift assay (EMSA) as described (Parikh et al., 2010a) with the dCRE1-containing oligonucleotide, 5′-AGCTAAAATATGACGTATTAACTTTT-3′ (dCRE1 sequence is indicated by boldface), and the mutated CRE oligonucleotide (mCRE), 5′-AGCTAAAATACACAAAATTAACTTTT-3′, (mutations are underlined). Oligonucleotide labeling, incubation, electrophoresis, and autoradiography were done as described (Parikh et al., 2010a).

RNA preparation and quantitative RT-PCR

We prepared total RNA using Trizol (Invitrogen) and treated the samples with DNaseI to remove residual genomic DNA. We subjected the RNA to reverse transcription using an oligo-dT primer and performed quantitative PCR on an Opticon3 system (MJ Research and Biorad) using gene-specific primer sets (Table S2). We used the Delta-Delta-Ct method to detect relative changes in RNA abundance (Schmittgen et al., 2000; Winer et al., 1999) against the reference gene IG7 (Bloomfield and Pears, 2003).

Spore and stalk purification

We collected spores from AX4 fruiting bodies using a metal loop. We then collected the remaining structures and washed the residual spores through a 40 μm cell strainer (BD falcon) to purify stalks.

Sporulation efficiency, detergent resistance and spore-germination efficiency

We collected all the fruiting bodies from a quarter nitrocellulose filter into 5 ml of 0.1% NP-40 and 1 mM EDTA in 20 mM potassium phosphate pH 6.2 (KK2). For sporulation efficiency, we counted the spores with phase-contrast microscopy. For detergent resistance, we plated spores on SM agar (at least 800 spores for AX4, 2000 for *bzpF*$^{-}$) in association with bacteria (*Klebsiella pneumoniae*) and counted plaques in the bacterial lawn after 3-6

days. For spore-germination efficiency, we collected sori from 2-day old fruiting bodies, resuspended them in HL5 at 2×10^6 cells/ml and shook them at 200 RPM for 6 hours at 22°C. We then counted the spores and the amoebae with phase-contrast microscopy. Germination efficiency is the ratio between germinated amoebae and the total cell number.

Spore staining

We collected spores from 30-hour fruiting bodies into 0.5 ml KK2 buffer. For staining with the fluorescent vital dye propidium iodide (PI; Sigma), we mixed the spores with 2.6 μg/ml propidium iodide and incubated at room temperature for 30 minutes (Levraud et al., 2003). We examined the spores by fluorescence microscopy and by flow cytometry with a BD Biosciences LSRII system equipped with a 488 nm argon laser. In some cases, we monitored GFP signals with the same equipment.

For lectin staining, we used FITC-labeled *Arachis hypogaea* lectin (Sigma) at a concentration of 40 μg/ml. After treating spores with or without urea (Wang et al., 2003), we incubated the spores with the FITC-lectin for 30 min at room temperature, washed them twice with KK2 buffer and examined the samples with fluorescence microscopy (Fosnaugh et al., 1994).

To stain for cellulose within the spore coat, we used Calcofluor white (Sigma). We incubated the spores with 0.01% (w/v) solution of Calcofluor in KK2 buffer at room temperature for 3-5 minutes. We washed the spores three times with KK2 buffer and examined the samples by fluorescence microscopy.

8-Br-cAMP-induction of sporulation

We developed cells on nitrocellulose filters for 19–20 hours, harvested the structures, dissociated them by repeated pipetting in EDTA-KK2 (Katoh et al., 2004) and washed them thrice with KK2. We induced sporulation as described (Wang et al., 1996) except for using 15 mM 8-Br-cAMP (Sigma) instead of 20 mM.

Induction of gene expression

We developed cells for 19 hours on filters, disassociated and resuspended them as above. We treated the cells with or without 20 mM 8-Br-cAMP for 2 hours at 22°C in Petri dishes. We then collected the cells and prepared RNA for quantitative RT-PCR analysis.

Computational analysis of potential BzpF target genes

We searched the *D. discoideum* genome for genes that contain at least one dCRE motif in the region between -600 to +150 relative to the ORF. We then calculated the target score according to two criteria: the BzpF-binding preference of the dCRE motifs and co-expression with *bzpF*. To find targets with high affinity for BzpF, we used the PBM assay binding preference results (Table S3, threshold > 0.4). We obtained the score of each putative target gene by summing the binding preference scores of all the dCRE motifs. The score was downweighted if the dCRE motifs were located in transcribed regions, according to the RNA-seq data. We used published expression data (Parikh et al., 2010b) to search for genes whose expression patterns correlate with that of *bzpF* during development. Using the Dynamic Time Warp (DTW) method (Sakoe and Chiba, 1978), we aligned the time course data with slightly shifted phases (±1 time point) to compare the time series of the expression levels and then used Pearson's correlation on the DTW-transformed expression profiles to evaluate the correlation with the *bzpF* expression pattern. To determine significance ($p < 0.15$), we permuted the BzpF binding preference scores among the 8-mers and repeated the analysis 30 times to obtain a null distribution. We used that distribution to determine the p-value of the experimental data.

RNA Sequencing

We collected RNA from cells at 25 hours of development and processed the samples as described (Parikh et al., 2010b), except that we performed the poly(A) selection twice. We analyzed the RNA-seq data using the data mining software Orange (Curk et al., 2005).

Results

bzpF encodes a CREB-like protein

bzpF was implicated as a CREB gene by transcriptional network analysis (Parikh et al., 2010a). To test this possibility, we analyzed the predicted BzpF protein sequence (631 amino acids) and found a PKA-phosphorylation consensus sites at S438, inside the bZIP region, and glutamine-rich Q-domains at the N-terminal region (Fig. 1A). However, the characteristic KID motif was not readily evident in BzpF. By BLAST search, we found that BzpF is similar to bZIP proteins in *Naegleria*, to the mammalian CREB3L3 and CREB3L1, and to the *Arabidopsis* bZIP49 and bZIP17 proteins, which belong to the CREB/ATF subfamily which is involved in ER stress response (Audas et al., 2008; Tajima et al., 2008). Nevertheless, BzpF does not have a putative transmembrane domain, which is characteristic of the CREB/ATF subfamily members (Llarena et al., 2010). We also found that BzpF has a close homolog in *Dictyostelium purpureum*. Therefore, we propose that BzpF is a Dictyostelid type CREB-like protein.

The *D. purpureum bzpF* gene model (DPU_G0065610; May 2011) in DictyBase predicted a 249-amino acids protein, 382 amino acids shorter than the *D. discoideum* BzpF. We assembled RNA-seq reads (Parikh et al., 2010b) and found an unidentified intron 47-bp upstream of the predicted start codon of the DictyBase gene model. In addition, we found three sequencing errors around the predicted stop codon. We predict that the *D. purpureum bzpF* gene encodes a 531–amino acids protein that has 64.1% identity and 69.9% similarity to the *D. discoideum* BzpF protein (Fig. S1). Most of the protein sequence, including the bZIP region at the C-terminus, are conserved in both BzpFs except for a poly-Asparagine sequences at the N-terminus of the *D. discoideum* protein.

BzpF binds the canonical CRE in vitro (Parikh et al., 2010a). To find the preferred DNA motif for BzpF, we tested the GST-fused bZIP region of BzpF (BzpFzip-GST, Fig. 1A) against a microarray that contains all possible 8-mer oligonucleotides. We show the result as a position weight matrix in Fig. 1B. We named the sequence, dCRE1, for which BzpFzip-GST had the highest preferences. dCRE1 differs by one nucleotide from the canonical CRE sequence, creating an asymmetric site (Fig. 1B). We confirmed the preference of BzpF to dCRE1 by EMSA. BzpFzip-GST bound the dCRE1-containing oligonucleotide (Fig. 1C, lane 3) but not a mutated oligonucleotide (mCRE; Fig. 1C, lane 7). The shifted band was super-shifted in the presence of an antibody against GST (Fig. 1C, lane 4), suggesting that the binding was indeed mediated by the BzpFzip-GST. We used the GST-fused bZIP region of DimA, which is a well-characterized *Dictyostelium* bZIP protein, as a control. This bZIP region did not bind the dCRE1-containing oligonucleotide (Fig. 1C, lane 2), indicating the binding specificity of BzpF to dCRE1. We also performed a competition assay by adding unlabeled oligonucleotides to the reaction. Increasing amounts of the mutated oligonucleotide had almost no effect (Fig. 1D, lanes 1-3), whereas the binding was decreased by the addition of unlabeled dCRE1 (Fig. 1D, lanes 4-6). These results suggest that BzpF binds to dCRE1 in a sequence-specific manner, extending the finding that BzpF binds to the canonical CRE (Parikh et al., 2010a).

bzpF is expressed preferentially in spores during late culmination

We examined the expression profile of *bzpF* during development by quantitative RT-PCR and by mining the developmental RNA-seq database (Parikh et al., 2010b). *bzpF* expression is not detectable at 0-12 hours of development. The mRNA is first detectable at 16 hours and it continues to accumulate through the end of development (Fig. 2A), suggesting a function during terminal differentiation. We also checked the expression of the *bzpF* ortholog in the related species *D. purpureum*. We observed a similar pattern of mRNA abundance with a slight temporal delay (Fig. 2A), as expected from the observation that *D. purpureum* develops more slowly than *D. discoideum* (Parikh et al., 2010b). The RNA-seq data also suggest that the *bzpF* mRNA is enriched in prestalk cells during slug migration, about 2-fold in *D. discoideum* and 4-fold in *D. purpureum* relative to prespore cells (Fig. 2B). To examine the cell-type specificity in fruiting bodies, where the transcript is at peak abundance, we purified spores and stalk cells and measured *bzpF* expression. We found that *bzpF* is expressed in both cell types, but it is enriched about 4 fold in the spores (Fig. 2C). By measuring the mRNA levels of the stalk specific gene *ecmA* (Harwood et al., 1993) and the spore specific gene *spiA* (Richardson et al., 1991) we found that the spore sample contains no more than 14.8% stalk RNA and the stalk sample contains no more than 2.0% spore RNA (Fig. 2C).

D. discoideum and *D. purpureum* have diverged approximately 400 million years ago (Sucgang et al., 2011). The similarity between the expression patterns of *bzpF* in these two organisms (Fig. 2A,B) suggests constant selective surveillance of this trait and an evolutionary conserved function. We propose that BzpF activity is required during late stages of development in both cell types, preferentially in the spores.

bzpF^{-} mutants produce compromised spores

To test the developmental role of *bzpF*, we generated a mutant by deleting most of the coding region (Fig. 1A). The mutant cells grow normally on bacteria and in HL5 liquid medium. During development on bacterial plates, the mutant exhibits aberrant fruiting-body morphology with thick, irregular stalks and light-colored, translucent sori (data not shown). We also developed axenically grown cells on nitrocellulose filters (Fig. 3A). Under these conditions, the *bzpF*$^{-}$ mutants are morphologically indistinguishable from the wild type during the first 16 hours. At the end of development the mutants exhibit asynchronous culmination. Fruiting body formation is completed at 28-30 hours and the stalks are short and thick (Fig. 3A a, c). The *bzpF*$^{-}$ sori appear abnormal – they are more translucent than those of the wild type (Fig. 3A c). Upon prolonged incubation, most of the mutant sori slipped down the stalks and the remaining sori become more translucent, while the AX4 sori become opaque and yellow (Fig. 3A b, d). These observations suggest that the support for sori is weak and that spore development and spore stability are compromised in the *bzpF*$^{-}$ strain.

We compared the spore stability of the *bzpF*$^{-}$ mutant to that of AX4 after several days of development. The spore number of the *bzpF*$^{-}$ mutant is only slightly lower than that of AX4 at 2 days, but it is markedly decreased after 3-5 days, suggesting spore instability (Fig. 3B). We also examined the detergent resistance of the spores and found that the *bzpF*$^{-}$ spores are much more sensitive than their AX4 counterparts (Fig. 3C), further suggesting spore instability. We note that the declines in spore count and in detergent resistance were not due to germination within the sori because we have not found hatched amoebae and empty spore shells in the mutant sori.

To test the potential cause of the spore instability, we examined whether the spore coat of the *bzpF*$^{-}$ spores is compromised. The *Dictyostelium* spore coat is composed of three layers;

the central mid layer, which includes galactose-rich polysaccharides and cellulose, is sandwiched between two protein-rich layers (West, 2003). A compromised outer layer could result in a porous, less protective spore coat (Fosnaugh et al., 1994) that can be detected by staining of mid layer components with a fluorescently-labeled lectin, which recognizes polysaccharides, and with calcofluor, which stains cellulose. The *bzpF*⁻ spores were stained slightly stronger than AX4 spores with both FITC-labeled lectins and with calcofluor (Fig. S2A and B). Stronger FITC-labeled lectin staining could also be caused by altered glycosylation level (Wang et al., 2003). We therefore treated the spores with urea permeabilization, which strips the external layer barrier proteins before the FITC-lectin staining. This experiment ruled out the possibility of altered N-glycosylation because the staining level of AX4 and *bzpF*⁻ spores were nearly identical after urea treatment (Fig. S2). Therefore, the stronger staining with FITC-lectin and calcofluor (Fig. S2A and B) indicates that the *bzpF*⁻ spore coat outer layer might be slightly compromised, possibly due to the loss of some urea-soluble components from the spore coat. The *bzpF*⁻ spores also have visible defects. Compared to the birefringent wild-type spores, most of the *bzpF*⁻ spores appear dark under phase-contrast microscopy (Fig. 4A). Viable spores can exclude propidium iodide (PI) (Cornillon et al., 1994; Yoshino et al., 2007) so we stained the spores with PI to monitor spore integrity. The difference between *bzpF*⁻ and AX4 is dramatic (Fig. 4A). The AX4 spores are almost completely free of PI staining (1.7% positive, Fig. 4B), whereas most of the *bzpF*⁻ spores are stained (78.1% positive, Fig. 4B). In addition, almost all of the stained spores are phase-dark (Fig. 4A), suggesting that the membrane of the *bzpF*⁻ spores is compromised.

Finally, we examined spore-germination by incubating the spores in liquid medium. The fraction of hatched amoebae in the *bzpF*⁻ population (18.4%, Fig. 4C) is lower than in AX4 (73.4%, Fig. 4C), consistent with the fraction of PI-negative, phase-bright spores in these strains.

Overall, the *bzpF*⁻ spores are compromised, most likely due to defects in the cell membrane inside the spore coat. We postulate that these defects lead to spore instability within the sori, resulting in reduced viability, detergent sensitivity, and poor germination.

Ectopic expression of *bzpF*

We fused the *bzpF* coding region with the GFP coding region and cloned the fusion gene under the ubiquitous *actin15* promoter (Fig. 5A). We transformed the *bzpF*⁻ strain with the expression vector and observed high but variable levels of *bzpF* mRNA in the transformants during growth (0 hours) and during late development (20 hours) (Fig. 5B). Western-blot analysis revealed small amounts of the full-size BzpF-GFP fusion protein and high amounts of apparent degradation products (data not shown). We then examined the spores of the transformants by flow cytometry and found that only about 10% are GFP positive (Fig. 5C). In contrast, *bzpF*⁻ cells transformed with a GFP vector alone show 85% GFP-positive spores (Fig. 5C). These results suggest that the BzpF-fusion protein may be unstable upon ectopic expression. Another possibility is the potential expression of a truncated BzpF peptide (1-137 amino acids) that may be produced as a consequence of the deletion in *bzpF*⁻. This potential peptide would lack the bZIP domain but it would carry a short conserved region (1-56 amino acids, see Fig. S1) that may have a dominant negative effect over the transgenic BzpF.

The availability of strains that produce 10% BzpF-GFP-positive spores allowed us to test whether ectopic expression of the BzpF-GFP fusion protein could complement some of the *bzpF*⁻ phenotypes. To test the compromised spore phenotype, we stained the spores with PI and used flow cytometry to simultaneously count GFP-positive and PI-positive spores. Almost none of the BzpF-GFP-expressing spores were stained with PI, similar to the level

observed in AX4, whereas most of the *bzpF*⁻ spores expressing GFP alone were stained with PI (Fig. 5D). Among the BzpF-GFP-negative spores in the same populations, almost all are stained with PI (Fig. 5E). These results suggest that ectopic expression of the BzpF-GFP fusion protein is sufficient to complement the *bzpF*⁻ mutation with respect to the spore instability phenotype. Expression of GFP alone is not a confounding factor and the partial penetrance of the ectopic expression system allows us to suggest that the complementation, and therefore the function of BzpF, are cell autonomous.

We also developed the transformed cells on nitrocellulose filters to test the effect of the ectopically-expressed fusion protein on morphogenesis. During the first 16 hours, the transformed cells develop normally, as do the *bzpF*⁻ cells. Later in development the BzpF-GFP transformants exhibit asynchronous culmination and aberrant fruiting bodies (Fig. 5F), also identical to the *bzpF*⁻ phenotypes (Fig. 3A) and different from AX4, suggesting that the overexpression vector is not capable of complementing the *bzpF*⁻ mutation with respect to developmental morphology. This failure to complement is probably due to the low proportion of cells (10%) that express the full-length fusion protein in the developing mass and to the cell-autonomous nature of the BzpF function.

PKA-C activation does not suppress the *bzpF*⁻ phenotype

Activation of PKA can suppress many developmental defects in *Dictyostelium*, indicating that PKA-C functions downstream of the mutated gene responsible for the defect (Loomis, 1998; Richardson and Loomis, 1992; Wang and Kuspa, 1997). Previous analyses implicated BzpF as a member of the PKA-pathway and suggested that it functions downstream of PKA-C (Parikh et al., 2010a), but our analysis shows that BzpF lacks several characteristic CREB domains so it might not function downstream of PKA. It was therefore of interest to test the relationship between PKA-C activation and *bzpF* function. We postulated that if BzpF functions downstream of PKA-C, then activation of PKA-C would not suppress the *bzpF*⁻ phenotype. 8-Br-cAMP is a membrane-permeable analogue of cAMP that activates PKA by dissociating the PKA-R regulatory subunit from the PKA-C catalytic subunit (Kay, 1989; Maeda, 1988). We developed AX4 and *bzpF*⁻ cells on filters for 19-20 hours, disaggregated the multicellular structures, incubated the cells with or without 15 mM 8-Br-cAMP, and measured the proportion of spores that have formed. In the control experiment, 75.2% of the treated AX4 cells sporulate in response to 8-Br-cAMP whereas *bzpF*⁻ achieves 46.5% sporulation, which is significantly lower (Student's t-test, $p=0.02$) (Fig. 6A). This finding suggests that activation of PKA-C is not sufficient to fully induce sporulation in the absence of BzpF. Neither strain produces a significant number of spores without 8-Br-cAMP (Fig. 6A).

We also tested the detergent resistance of the induced spores. The *bzpF*⁻ spores have very low detergent resistance (Fig. 6B), similar to the level observed after filter development (Fig. 3D), whereas the AX4 spores are detergent resistant (Fig. 6B). These findings indicate that activation of PKA-C does not suppress the defects of the *bzpF*⁻ strain. We suggest that PKA-C is not downstream of BzpF in a pathway that regulates sporulation, which is consistent with the idea that BzpF functions downstream of PKA-C or that the two proteins function in parallel pathways.

The transcriptional targets of BzpF

If BzpF is a transcription factor, it should be both necessary and sufficient for the expression of genes that contain its binding motifs in their promoters. We searched the *Dictyostelium* genome (Eichinger et al., 2005) for genes that carry any one of the dCRE motifs (Table S3) in their potential promoter regions and found 1197 candidates. We narrowed the list down using computational and experimental approaches. First, we postulated that the expression

of BzpF-target genes would be changed after *bzpF* is expressed, so we searched the *Dictyostelium* wild type transcriptome (Parikh et al., 2010b) for genes whose developmental expression correlates well with that of *bzpF*. Second, we calculated the score of each putative target gene following two criteria: the BzpF-binding preference from the PBM assay results and the co-expression with *bzpF*. We found 18 genes whose promoter regions include dCRE motifs with high binding affinities and whose expression patterns were positively correlated (Pearson's $r > 0.8$) with *bzpF* during development (Table S4). There is no gene with negative correlation ($r < –0.8$) with *bzpF*. To find additional potential target genes of BzpF, we also performed RNA-seq on late-stage AX4 and *bzpF*$^{–}$ samples (Dataset S2) and found 13 additional genes that have at least one dCRE motif (with a lower stringency than the above criteria) and show reduced expression in *bzpF*$^{–}$ (Table S5). We also checked whether the other 18 genes exhibit differential expression in the mutant strain and found that 11 were indeed expressed at a lower level in *bzpF*$^{–}$ (Table S4).

Next, we examined whether the expression of those genes is induced by activation of PKA-C in a BzpF-dependent manner. We chose 11 genes, including *bzpF*, from the first approach (Table S4, bold font) and 5 genes from the second approach (Table S5, bold font) and performed quantitative RT-PCR on 8-Br-cAMP-treated samples. Expression of 15 of the 16 genes is inducible by 8-Br-cAMP in AX4 (Fig. 7) and all 15 are less abundant in the *bzpF*$^{–}$ mutant. The prespore genes, *cotB* and *spiA*, which are known to be regulated by PKA, are induced to almost the same level in both strains, suggesting that the PKA-pathway in *bzpF*$^{–}$ can be activated by 8-Br-cAMP. These data indicate that BzpF is necessary for the transcriptional activation of several terminal differentiation genes that are also regulated by the PKA pathway. These 15 genes are potential direct targets of BzpF.

We also tested whether BzpF is sufficient for the transcriptional activation of the putative target genes. Since these target genes are not expressed in vegetative cells, we measured mRNA abundance in vegetative cells that express BzpF ectopically. We prepared RNA from vegetatively growing *bzpF*$^{–}$ and a BzpF-GFP transformant. Using quantitative RT-PCR we found an increase in the expression of 2 putative target genes in the BzpF-overexpressing strain relative to *bzpF*$^{–}$ (Fig. 8), suggesting that BzpF is both necessary and sufficient for the expression of these two genes.

The results shown in Figs 7 and 8 supported the idea that BzpF is a transcription factor because it is both necessary and sufficient for the transcriptional activation of its target genes.

Biological processes regulated by BzpF

Comparing the transcriptomes of the *bzpF*$^{–}$ mutant and the wild type revealed 205 genes that are under-expressed in *bzpF*$^{–}$ ($\log_2$(AX4/*bzpF*$^{–}$)>1, AX4 raw read count>100). Only 24 of the genes contain dCRE in their upstream regions, so we suspect that most of these transcriptional changes are secondary consequences of the mutation. The genes encode 13 cellulose-binding domain-containing proteins, 4 spore germination proteins, and 3 GATA transcription factors (Table S6). We also checked the differential expression of cell-type marker genes (Parikh et al., 2010b) between the wild type strain AX4 and the *bzpF*$^{–}$ mutants. We found that 19 out of 633 prespore genes and 22 out of 800 prestalk genes exhibit differential expression (Table S7). In *bzpF*$^{–}$, the expression levels of *cotA, B and C*, which are prespore markers, are not significantly different from those in AX4 (*cotA, B and C* $\log_2$(AX4/*bzpF*$^{–}$)= 0.58, 0.05, 0.12, respectively). The expression level of *cotE*, which encodes a spore coat protein, is greatly decreased in the *bzpF*$^{–}$ strain ($\log_2$(AX4/*bzpF*$^{–}$)= 1.72) (Table S6 and S7). The expression of *ecmA*, which a prestalk markers, exhibited almost no difference ($\log_2$(AX4/*bzpF*$^{–}$)= 0.21). On the other hand, the expression level of another prestalk marker, *ecmB*, in the *bzpF*$^{–}$ strain is less than half of the wild type level

($\log_2$(AX4/*bzpF*$^-$)= 1.03). These data suggest that BzpF might be involved in both cell-type differentiation processes – stalk differentiation and late spore maturation through direct or indirect transcriptional regulation of developmental genes. A Gene Ontology (GO) enrichment analysis of the 205 genes is shown in Table 1. These Genes are enriched in the GO categories “lipid biosynthesis” and “fatty acid biosynthesis”. The most differentially expressed genes ($\log_2$(AX4/*bzpF*$^-$)>3) are enriched in “cellulose binding” and “sugar binding” (Table 1).

Discussion

Our studies show that BzpF is a CREB-like transcription factor, which functions downstream of PKA-pathway and regulates spore maturation and stability during late *Dictyostelium* development. BzpF binds the canonical CRE motif as well as the related dCRE motif.

Dictyostelium spores have a thick spore coat layer, which contains proteins and polysaccharides. The spore coat proteins and the galactose-rich polysaccharides first accumulate in prespore vesicles during early-mid development and are secreted by exocytosis under the control of PKA at the beginning of sporulation. Subsequently, cellulose is synthesized and extruded from the cells to form the mid layer, which is sandwiched by protein-rich outer and inner layers. The cellulose layer interacts with the coat glycoproteins to form a protein-impermeability barrier (West, 2003; West et al., 2009). Spore integrity could be compromised at many levels, including defects in the cellulose layer and the galactose rich polysaccharides layer, glycosylation defects, and inner membrane defects. The loss of BzpF causes severe spore defects that are manifested as spore instability and low germination efficiency. Genes that are down regulated in the mutant are involved in lipid and fatty acid biosynthesis as well as cellulose and sugar-binding, although most of these genes are probably not regulated directly by BzpF. These findings suggest that BzpF affects membrane biosynthesis and spore coat formation through indirect transcriptional regulation of cellulose and sugar binding proteins, which in turn promote maturation of spores and maintenance of their dormancy (Fig. 9). Some of the BzpF targets we have identified are members of the GATA transcription factor gene family, so it is possible that BzpF regulates a sporulation-specific cascade of transcriptional events.

Another essential factor of sporulation is the MADS-box transcription factor SrfA (Escalante and Sastre, 1998, 2002). Loss of this gene results in spores that are round and phase-dark. These spores have reduced calcofluor staining and reduced expression of *spiA*, which encodes a late spore coat protein. PKA activity leads to *srfA* expression during culmination and SrfA regulates *spiA* expression indirectly (Fig. 9). Unlike *srfA*$^-$ spores, *bzpF*$^-$ spores are oval and well-stained with calcofluor, even though they are phase-dark. Moreover, the expression of *cotB*, *spiA* and *srfA* in *bzpF*$^-$ is almost indistinguishable from the wild type, suggesting that BzpF and SrfA have largely parallel roles in the regulation of sporulation (Fig. 9). Nevertheless, there might be some overlap between the two pathways because the expression of six SrfA-induced genes (*sigL-1*, *rnpA*, *sigK*, *sigM*, *sigD* and *sigI*) is significantly lower in *bzpF*$^-$ than in AX4 and three of the genes contain dCRE motifs in their promoter regions (Fig. 9, Table S6). In many cases, the expression levels of developmental genes might be regulated by the coordination of multiple transcription factors.

In *Dictyostelium* development, PKA plays pivotal roles in the control of transcriptional regulation during multiple processes, including aggregation, prespore/prestlak differentiation and spore maturation. BzpF acts downstream of PKA, but, it is not expressed at aggregation stage. Other transcription factors, including other bZIP proteins such as *bzpD* and *bzpH*,

which are expressed at the early stages, may transduce the PKA signals to regulate developmental gene expression. The expression of *bzpF* is initially detected at 16 hrs in both cell types. It is enriched in prestalk cells during slug migration and then accumulates in spores during culmination. Consistent with this observation, the *bzpF*$^{-}$ mutant exhibits two stalk-related phenotypes in addition to the severe spore defects: thick stalks and weak support of the lower cup, which results in slippage of the sori down the stalk. Also, some of the target genes of BzpF are preferentially expressed in prestalk cells (Table S6, S7). The prestalk marker genes *aslA-1* and *ecmB*, which are normally expressed in the upper and lower cups during culmination, are down-regulated in *bzpF*$^{-}$ (Table S7), suggesting that they might be indirect targets of BzpF and their down-regulation may be related to the weak lower cup support phenotype. We propose that BzpF regulates two developmental processes – early prestalk differentiation and late spore maturation – raising the possibility that BzpF interacts with different components in those cell types. The fact that the 19 *Dictyostelium* bZIP proteins can form various homo- and hetero-dimers (Deppmann et al., 2006; Huang et al., 2006) suggests that BzpF may dimerize with other bZIP proteins in the different cell types and such hetero-dimer complexes may have specific roles and targets.

Based on sequence analysis, BzpF is neither a canonical CREB nor a classical CREB3 type protein. Our results suggest that BzpF may function downstream of PKA-C in *D. discoideum* although we have no conclusive evidence that it is directly regulated by PKA-C through phosphorylation. Future studies will be needed to determine whether PKA regulates BzpF and how BzpF regulates the transcription of each target gene we found here. Nevertheless, BzpF is a CREB-like transcription factors because it binds dCRE1, a motif only 1-bp different from the mammalian CRE, and it functions in concert with PKA-C to regulate terminal differentiation in *Dictyostelium*.

Supplementary Material

Refer to Web version on PubMed Central for supplementary material.

Acknowledgments

We thank A. Parikh for assistance with the RNA-seq data analysis, I. Mann, E. Chan, and H. van Bakel for technical and computational support, and A. Kuspa for useful discussions. We are grateful to the Dicty stock center for vectors. This work was supported by grants from the National Institute of Child Health and Human Development (P01 HD39691), the Slovenian Research Agency (P2-0209, J2-2197, L2-1112, Z7-3665) and the Canadian Institutes of Health Research (MOP-77721).

References

Adachi H, Hasebe T, Yoshinaga K, Ohta T, Sutoh K. Isolation of *Dictyostelium discoideum* cytokinesis mutants by restriction enzyme-mediated integration of the blasticidin S resistance marker. Biochem Biophys Res Commun. 1994; 205:1808–1814. [PubMed: 7811269]

Audas TE, Li Y, Liang G, Lu R. A novel protein, Luman/CREB3 recruitment factor, inhibits Luman activation of the unfolded protein response. Mol Cell Biol. 2008; 28:3952–3966. [PubMed: 18391022]

Berger MF, Badis G, Gehrke AR, Talukder S, Philippakis AA, Pena-Castillo L, Alleyne TM, Mnaimneh S, Botvinnik OB, Chan ET, Khalid F, Zhang W, Newburger D, Jaeger SA, Morris QD, Bulyk ML, Hughes TR. Variation in homeodomain DNA binding revealed by high-resolution analysis of sequence preferences. Cell. 2008; 133:1266–1276. [PubMed: 18585359]

Berger MF, Philippakis AA, Qureshi AM, He FS, Estep PW 3rd, Bulyk ML. Compact, universal DNA microarrays to comprehensively determine transcription-factor binding site specificities. Nat Biotechnol. 2006; 24:1429–1435. [PubMed: 16998473]

Bloomfield G, Pears C. Superoxide signalling required for multicellular development of *Dictyostelium*. J Cell Sci. 2003; 116:3387–3397. [PubMed: 12840076]

Chin KT, Zhou HJ, Wong CM, Lee JM, Chan CP, Qiang BQ, Yuan JG, Ng IO, Jin DY. The liver-enriched transcription factor CREB-H is a growth suppressor protein underexpressed in hepatocellular carcinoma. Nucleic Acids Res. 2005; 33:1859–1873. [PubMed: 15800215]

Cornillon S, Foa C, Davoust J, Buonavista N, Gross JD, Golstein P. Programmed cell death in *Dictyostelium*. J Cell Sci. 1994; 107(Pt 10):2691–2704. [PubMed: 7876338]

Curk T, Demsar J, Xu Q, Leban G, Petrovic U, Bratko I, Shaulsky G, Zupan B. Microarray data mining with visual programming. Bioinformatics. 2005; 21:396–398. [PubMed: 15308546]

Dang CV, McGuire M, Buckmire M, Lee WM. Involvement of the 'leucine zipper' region in the oligomerization and transforming activity of human c-myc protein. Nature. 1989; 337:664–666. [PubMed: 2645525]

Deppmann CD, Alvania RS, Taparowsky EJ. Cross-species annotation of basic leucine zipper factor interactions: Insight into the evolution of closed interaction networks. Mol Biol Evol. 2006; 23:1480–1492. [PubMed: 16731568]

Eichinger L, Pachebat JA, Glockner G, Rajandream MA, Sucgang R, Berriman M, Song J, Olsen R, Szafranski K, Xu Q, Tunggal B, Kummerfeld S, Madera M, Konfortov BA, Rivero F, Bankier AT, Lehmann R, Hamlin N, Davies R, Gaudet P, Fey P, Pilcher K, Chen G, Saunders D, Sodergren E, Davis P, Kerhornou A, Nie X, Hall N, Anjard C, Hemphill L, Bason N, Farbrother P, Desany B, Just E, Morio T, Rost R, Churcher C, Cooper J, Haydock S, van Driessche N, Cronin A, Goodhead I, Muzny D, Mourier T, Pain A, Lu M, Harper D, Lindsay R, Hauser H, James K, Quiles M, Madan Babu M, Saito T, Buchrieser C, Wardroper A, Felder M, Thangavelu M, Johnson D, Knights A, Loulseged H, Mungall K, Oliver K, Price C, Quail MA, Urushihara H, Hernandez J, Rabbinowitsch E, Steffen D, Sanders M, Ma J, Kohara Y, Sharp S, Simmonds M, Spiegler S, Tivey A, Sugano S, White B, Walker D, Woodward J, Winckler T, Tanaka Y, Shaulsky G, Schleicher M, Weinstock G, Rosenthal A, Cox EC, Chisholm RL, Gibbs R, Loomis WF, Platzer M, Kay RR, Williams J, Dear PH, Noegel AA, Barrell B, Kuspa A. The genome of the social amoeba *Dictyostelium discoideum*. Nature. 2005; 435:43–57. [PubMed: 15875012]

Escalante R, Sastre L. A Serum Response Factor homolog is required for spore differentiation in *Dictyostelium*. Development. 1998; 125:3801–3808. [PubMed: 9729488]

Escalante R, Sastre L. Regulated expression of the MADS-box transcription factor SrfA mediates activation of gene expression by protein kinase A during *Dictyostelium* sporulation. Mech Dev. 2002; 117:201–208. [PubMed: 12204259]

Faix J, Kreppel L, Shaulsky G, Schleicher M, Kimmel AR. A rapid and efficient method to generate multiple gene disruptions in *Dictyostelium discoideum* using a single selectable marker and the Cre-loxP system. Nucleic Acids Res. 2004; 32:e143. [PubMed: 15507682]

Fosnaugh K, Fuller D, Loomis WF. Structural roles of the spore coat proteins in *Dictyostelium discoideum*. Dev Biol. 1994; 166:823–825. [PubMed: 7813801]

Gonzalez GA, Menzel P, Leonard J, Fischer WH, Montminy MR. Characterization of motifs which are critical for activity of the cyclic AMP-responsive transcription factor CREB. Mol Cell Biol. 1991; 11:1306–1312. [PubMed: 1671708]

Grove CA, De Masi F, Barrasa MI, Newburger DE, Alkema MJ, Bulyk ML, Walhout AJ. A multiparameter network reveals extensive divergence between *C. elegans* bHLH transcription factors. Cell. 2009; 138:314–327. [PubMed: 19632181]

Harwood AJ, Early A, Williams JG. A repressor controls the timing and spatial localisation of stalk cell-specific gene expression in *Dictyostelium*. Development. 1993; 118:1041–1048. [PubMed: 8269839]

Huang E, Blagg SL, Keller T, Katoh M, Shaulsky G, Thompson CR. bZIP transcription factor interactions regulate DIF responses in *Dictyostelium*. Development. 2006; 133:449–458. [PubMed: 16410410]

Johannessen M, Delghandi MP, Moens U. What turns CREB on? Cell Signal. 2004; 16:1211–1227. [PubMed: 15337521]

Katoh M, Shaw C, Xu Q, Van Driessche N, Morio T, Kuwayama H, Obara S, Urushihara H, Tanaka Y, Shaulsky G. An orderly retreat: Dedifferentiation is a regulated process. Proc Natl Acad Sci U S A. 2004; 101:7005–7010. [PubMed: 15103019]

Kay RR. Evidence that elevated intracellular cyclic AMP triggers spore maturation in *Dictyostelium*. Development. 1989; 105:753–759.

Kondo S, Murakami T, Tatsumi K, Ogata M, Kanemoto S, Otori K, Iseki K, Wanaka A, Imaizumi K. OASIS, a CREB/ATF-family member, modulates UPR signalling in astrocytes. Nat Cell Biol. 2005; 7:186–194. [PubMed: 15665855]

Kuspa A, Loomis WF. Tagging developmental genes in *Dictyostelium* by restriction enzyme-mediated integration of plasmid DNA. Proc Natl Acad Sci U S A. 1992; 89:8803–8807. [PubMed: 1326764]

Lam KN, van Bakel H, Cote AG, van der Ven A, Hughes TR. Sequence specificity is obtained from the majority of modular C2H2 zinc-finger arrays. Nucleic Acids Res. 2011

Levi S, Polyakov M, Egelhoff TT. Green fluorescent protein and epitope tag fusion vectors for *Dictyostelium discoideum*. Plasmid. 2000; 44:231–238. [PubMed: 11078649]

Levraud JP, Adam M, Luciani MF, de Chastellier C, Blanton RL, Golstein P. *Dictyostelium* cell death: early emergence and demise of highly polarized paddle cells. J Cell Biol. 2003; 160:1105–1114. [PubMed: 12654899]

Llarena M, Bailey D, Curtis H, O'Hare P. Different mechanisms of recognition and ER retention by transmembrane transcription factors CREB-H and ATF6. Traffic. 2010; 11:48–69. [PubMed: 19883396]

Loomis WF. Role of PKA in the timing of developmental events in *Dictyostelium* cells. Microbiol Mol Biol Rev. 1998; 62:684–694. [PubMed: 9729606]

Maeda M. Dual Effects of cAMP on the Stability of Prespore Vesicles and 8-bromo CAMP-enhanced Maturation of Spore and Stalk Cells of *Dictyostelium discoideum*. Develop Growth & Differ. 1988; 30:573–587.

Mengus G, Fadloun A, Kobi D, Thibault C, Perletti L, Michel I, Davidson I. TAF4 inactivation in embryonic fibroblasts activates TGF beta signalling and autocrine growth. EMBO J. 2005; 24:2753–2767. [PubMed: 16015375]

Montminy MR, Sevarino KA, Wagner JA, Mandel G, Goodman RH. Identification of a cyclic-AMP-responsive element within the rat somatostatin gene. Proc Natl Acad Sci U S A. 1986; 83:6682–6686. [PubMed: 2875459]

Murakami T, Saito A, Hino S, Kondo S, Kanemoto S, Chihara K, Sekiya H, Tsumagari K, Ochiai K, Yoshinaga K, Saitoh M, Nishimura R, Yoneda T, Kou I, Furuichi T, Ikegawa S, Ikawa M, Okabe M, Wanaka A, Imaizumi K. Signalling mediated by the endoplasmic reticulum stress transducer OASIS is involved in bone formation. Nat Cell Biol. 2009; 11:1205–1211. [PubMed: 19767743]

O'Shea EK, Rutkowski R, Kim PS. Evidence that the leucine zipper is a coiled coil. Science. 1989; 243:538–542. [PubMed: 2911757]

Omori Y, Imai J, Suzuki Y, Watanabe S, Tanigami A, Sugano S. OASIS is a transcriptional activator of CREB/ATF family with a transmembrane domain. Biochem Biophys Res Commun. 2002; 293:470–477. [PubMed: 12054625]

Omori Y, Imai J, Watanabe M, Komatsu T, Suzuki Y, Kataoka K, Watanabe S, Tanigami A, Sugano S. CREB-H: a novel mammalian transcription factor belonging to the CREB/ATF family and functioning via the box-B element with a liver-specific expression. Nucleic Acids Res. 2001; 29:2154–2162. [PubMed: 11353085]

Parikh A, Huang E, Dinh C, Zupan B, Kuspa A, Subramanian D, Shaulsky G. New components of the *Dictyostelium* PKA pathway revealed by Bayesian analysis of expression data. BMC Bioinformatics. 2010a; 11:163. [PubMed: 20356373]

Parikh A, Miranda ER, Katoh-Kurasawa M, Fuller D, Rot G, Zagar L, Curk T, Sucgang R, Chen R, Zupan B, Loomis WF, Kuspa A, Shaulsky G. Conserved developmental transcriptomes in evolutionarily divergent species. Genome Biol. 2010b; 11:R35. [PubMed: 20236529]

Richardson DL, Hong CB, Loomis WF. A prespore gene, Dd31, expressed during culmination of *Dictyostelium discoideum*. Dev Biol. 1991; 144:269–280. [PubMed: 2010032]

Richardson DL, Loomis WF. Disruption of the sporulation-specific gene spiA in *Dictyostelium discoideum* leads to spore instability. Genes Dev. 1992; 6:1058–1070. [PubMed: 1592257]

Sakoe H, Chiba S. Dynamic programming algorithm optimization for spoken word recognition. IEEE Transactions on Acoustics, Speech, and Signal Processing. 1978; 26:43–49.

Saran S, Meima ME, Alvarez-Curto E, Weening KE, Rozen DE, Schaap P. cAMP signaling in *Dictyostelium*. Complexity of cAMP synthesis, degradation and detection. J Muscle Res Cell Motil. 2002; 23:793–802. [PubMed: 12952077]

Schmittgen TD, Zakrajsek BA, Mills AG, Gorn V, Singer MJ, Reed MW. Quantitative reverse transcription-polymerase chain reaction to study mRNA decay: comparison of endpoint and real-time methods. Anal Biochem. 2000; 285:194–204. [PubMed: 11017702]

Shaulsky G, Loomis WF. Cell type regulation in response to expression of ricin A in *Dictyostelium*. Dev Biol. 1993; 160:85–98. [PubMed: 8224551]

Sucgang R, Kuo A, Tian X, Salerno W, Parikh A, Feasley CL, Dalin E, Tu H, Huang E, Barry K, Lindquist E, Shapiro H, Bruce D, Schmutz J, Salamov A, Fey P, Gaudet P, Anjard C, Mohan MB, Basu S, Bushmanova Y, van der Wel H, Katoh-Kurasawa M, Dinh C, Coutinho PM, Saito T, Elias M, Schaap P, Kay RR, Henrissat B, Eichinger L, Rivero F, Putnam NH, West CM, Loomis WF, Chisholm R, Shaulsky G, Strassmann JE, Queller DC, Kuspa A, Grigoriev I. Comparative genomics of the social amoebae *Dictyostelium discoideum* and *Dictyostelium purpureum*. Genome Biol. 2011; 12:R20. [PubMed: 21356102]

Sussman M. Cultivation and synchronous morphogenesis of *Dictyostelium* under controlled experimental conditions. Methods Cell Biol. 1987; 28:9–29. [PubMed: 3298997]

Tajima H, Iwata Y, Iwano M, Takayama S, Koizumi N. Identification of an Arabidopsis transmembrane bZIP transcription factor involved in the endoplasmic reticulum stress response. Biochem Biophys Res Commun. 2008; 374:242–247. [PubMed: 18634751]

Wang B, Kuspa A. *Dictyostelium* development in the absence of cAMP. Science. 1997; 277:251–254. [PubMed: 9211856]

Wang N, Shaulsky G, Escalante R, Loomis WF. A two-component histidine kinase gene that functions in *Dictyostelium* development. EMBO J. 1996; 15:3890–3898. [PubMed: 8670894]

Wang F, Metcalf T, van der Wel H, West CM. Initiation of mucin-type O-glycosylation in dictyostelium is homologous to the corresponding step in animals and is important for spore coat function. J Biol Chem. 2003; 278:51395–51407. [PubMed: 14551185]

West CM. Comparative analysis of spore coat formation, structure, and function in *Dictyostelium*. Int Rev Cytol. 2003; 222:237–293. [PubMed: 12503851]

West CM, Nguyen P, van der Wel H, Metcalf T, Sweeney KR, Blader IJ, Erdos GW. Dependence of stress resistance on a spore coat heteropolysaccharide in *Dictyostelium*. Eukaryot Cell. 2009; 8:27–36. [PubMed: 18996984]

Winer J, Jung CK, Shackel I, Williams PM. Development and validation of real-time quantitative reverse transcriptase-polymerase chain reaction for monitoring gene expression in cardiac myocytes in vitro. Anal Biochem. 1999; 270:41–49. [PubMed: 10328763]

Yoshino R, Morio T, Yamada Y, Kuwayama H, Sameshima M, Tanaka Y, Sesaki H, Iijima M. Regulation of ammonia homeostasis by the ammonium transporter AmtA in *Dictyostelium discoideum*. Eukaryot Cell. 2007; 6:2419–2428. [PubMed: 17951519]

Zhang K, Shen X, Wu J, Sakaki K, Saunders T, Rutkowski DT, Back SH, Kaufman RJ. Endoplasmic reticulum stress activates cleavage of CREBH to induce a systemic inflammatory response. Cell. 2006; 124:587–599. [PubMed: 16469704]

Highlights

- *Dictyostelium* bZIP protein BzpF binds to CRE-like sequence with high specificity.
- *bzpF* is expressed preferentially in spores during late culmination stage.
- Loss of BzpF results in severe defects in spore maturation and stability.
- We found 15 PKA-regulated, late-developmental genes as potential BzpF direct targets.
- Many under-expressed genes in *bzpF*$^{-}$ encode cellulose- and sugar-binding proteins.

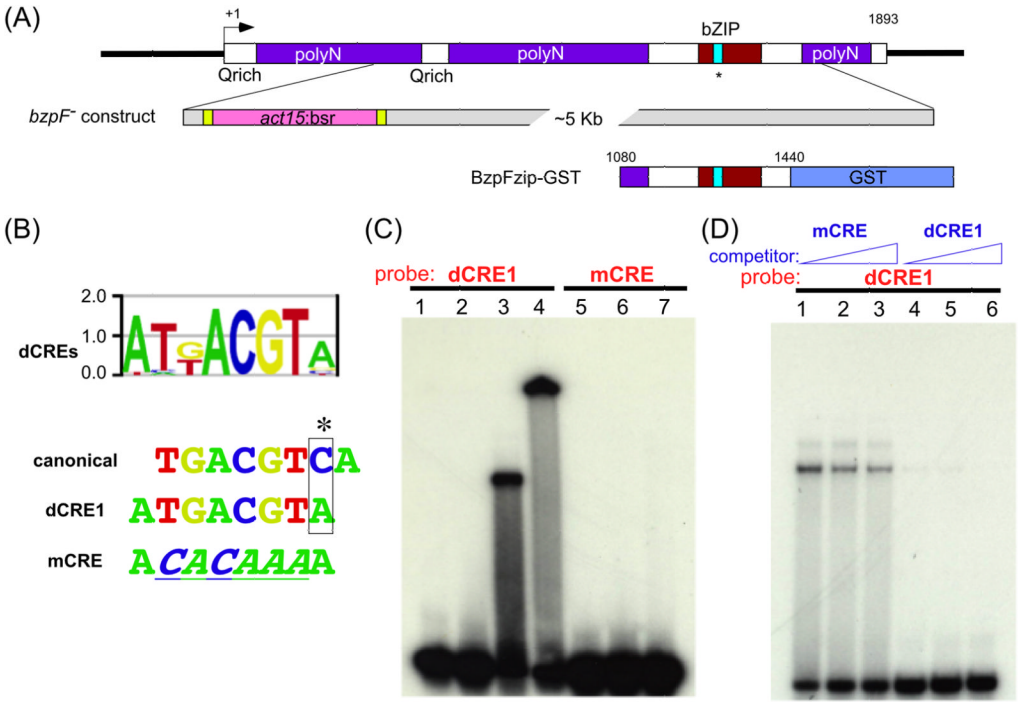

Fig. 1. *bzpF* is a CREB-like gene

(A) *A schematic representation of bzpF*: This single-exon gene is 1893 bp-long with multiple poly-N (purple boxes) and Q-rich coding regions. The bZIP domain (red box) is close to the carboxyl terminus; the cyan colored region inside the bZIP domain indicates a potential CRE binding domain, and the asterisk represents the PKA phosphorylation consensus site. *The bzpF⁻ construct*: The majority of the coding region (+414 to +1654) is replaced by a Blasticidin S resistance (bsr) cassette (pink), which is flanked by *loxP* recombination sites (yellow) and a plasmid backbone (grey). *The BzpFzip-GST construct*: The C-terminal region (+1080 to +1440) including the bZIP domain is fused with GST.

(B) *The DNA binding motif of BzpF:* An oligonucleotide-chip containing all possible 8 mers was used to measure the BzpF binding preference. The DNA sequences (dCREs) bound by BzpFzip-GST *in vitro* are summarized in a position weight matrix, which is shown as a sequence logo (Berger et al., 2006). The matrix includes the canonical CRE (canonical) and the sequence with the highest affinity for BzpF (dCRE1). The mutated-CRE oligonucleotide (mCRE) differs by 6 nucleotides from the dCRE1 sequence. The mutated nucleotides are underlined and italicized.

(C) *Electrophoresis mobility shift assay:* Radioactively labeled dCRE1-containing oligonucleotides (lanes 1-4) and mCRE-containing oligonucleotides (negative control: lanes 5-7) were used as probes. Lane 1 and 5 – no protein added; lane 2 and 6 – a control bZIP protein (DimAzip-GST); lanes 3 and 7 – BzpFzip-GST protein; lane 4 – BzpFzip-GST with anti-GST antibody. (D) *Competition EMSA:* We added unlabeled nonspecific mCRE (lanes 1-3; 20, 100 and 500 fold excess, respectively) or specific dCRE1 (lanes 4-6; 20, 100 and 500 fold excess, respectively) to the mixture of BzpFzip-GST and the radiolabeled dCRE1.

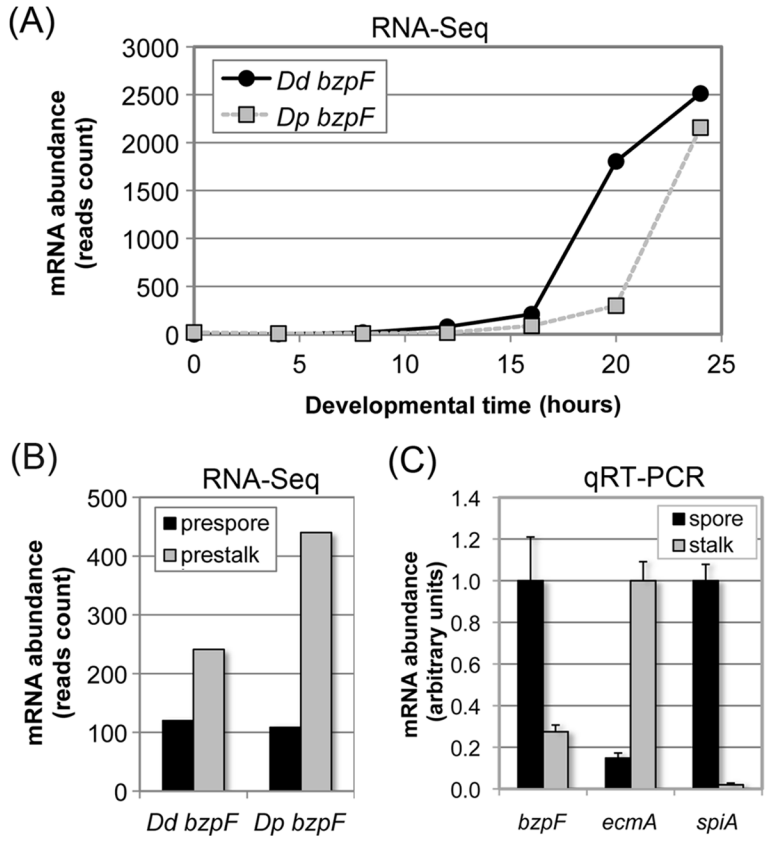

Fig. 2. *bzpF* is expressed during late development in *D. discoideum* and *D. purpureum*

(A) *The expression profile of bzpF during development*: Adapted from the published RNA-sequencing data of *D. discoideum* (*Dd bzpF*, black circles) and *D. purpureum* (*Dp bzpF*, grey squares) (Parikh et al., 2010b). Time points (hours) are indicated on the x-axis and mRNA abundance (normalized read-counts) on the y-axis.

(B) *Preferential expression of bzpF in prestalk cells*: Adapted from the published RNA-sequencing data of *D. discoideum* (*Dd bzpF*) and *D. purpureum* (*Dp bzpF*) (Parikh et al., 2010b). *bzpF* mRNA is detectable in both prespore cells (black bars) and prestalk cells (gray bars) in slugs. The y-axis indicates mRNA abundance (normalized read counts). (C) *Preferential expression of bzpF in spores:* We performed quantitative RT-PCR on RNA from spores (black bars) and stalk cells (grey bars) enriched from mature *D. discoideum* fruiting bodies. The enrichment of the isolated cell types is illustrated with the stalk-specific marker *ecmA* and the spore-specific marker *spiA*. The sample with the most abundant mRNA was normalized to 1 unit (y-axis) for each gene. The data are represented as mean + s.e.m of four replicates.

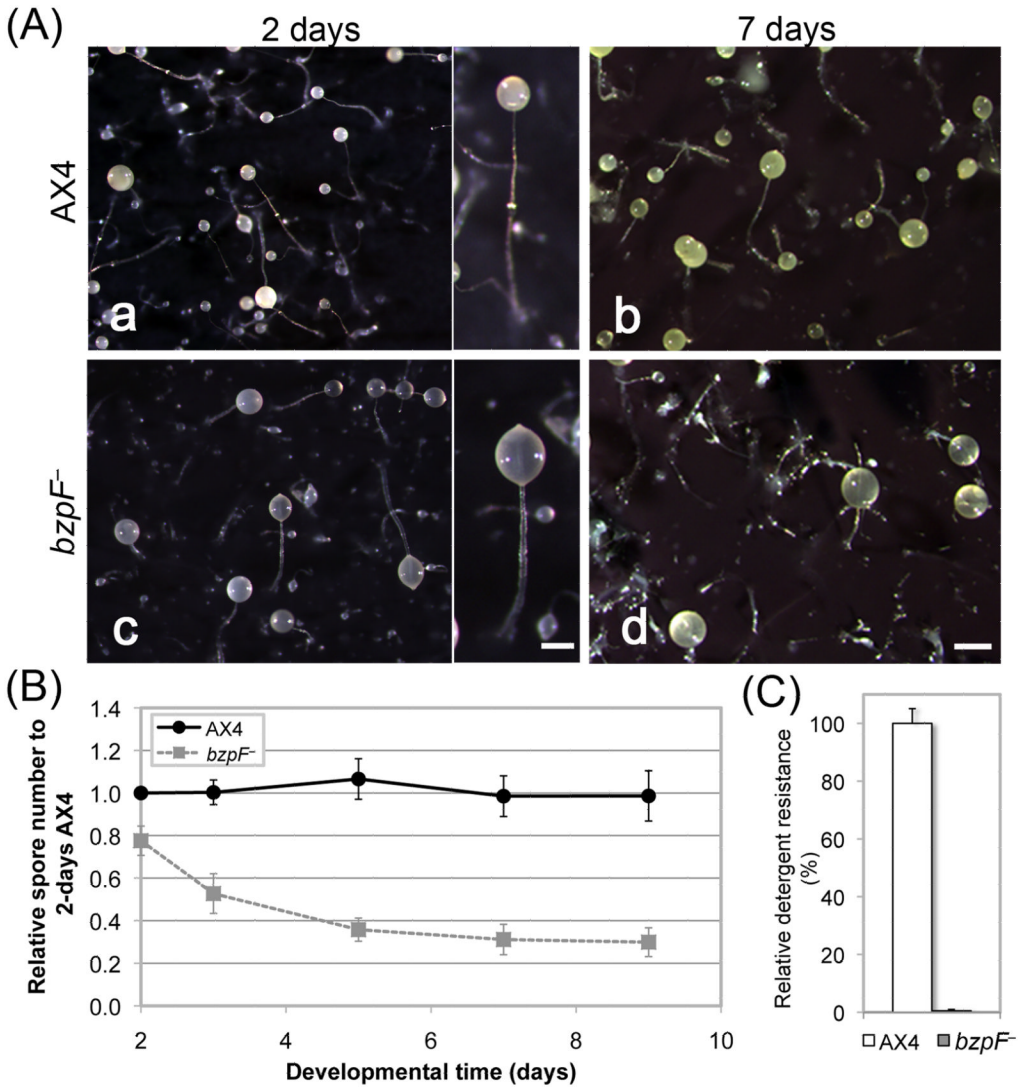

Fig. 3. *bzpF*⁻ cells exhibit morphological defects during development

(A) *Morphology:* We developed cells for 2 and 7 days on dark filters and photographed the multicellualr structures of AX4 (a and b, respectively) and the *bzpF*⁻ mutant (c and d, respectively). Bar = 0.2 mm in the magnified image, 0.5 mm in d. (B) *Spore stability:* We counted spores (AX4 - circles, solid line; *bzpF*⁻ - squares, dashed line) between 2 - 9 days of incubation on filters (x-axis) as a fraction of the value observed for AX4 at 2 days (y-axis). The data are the means ± s.e.m of four replicates. (C) *Detergent resistance:* We incubated AX4 spores (white bar) and *bzpF*⁻ spores (grey bar) in 0.1% NP-40 and plated them on nutrient agar in association with bacteria. The number of plaques formed on the bacterial lawn relative to the number of spores plated (%) is the detergent resistance (y-axis). The data are the means + s.e.m of three replicates.

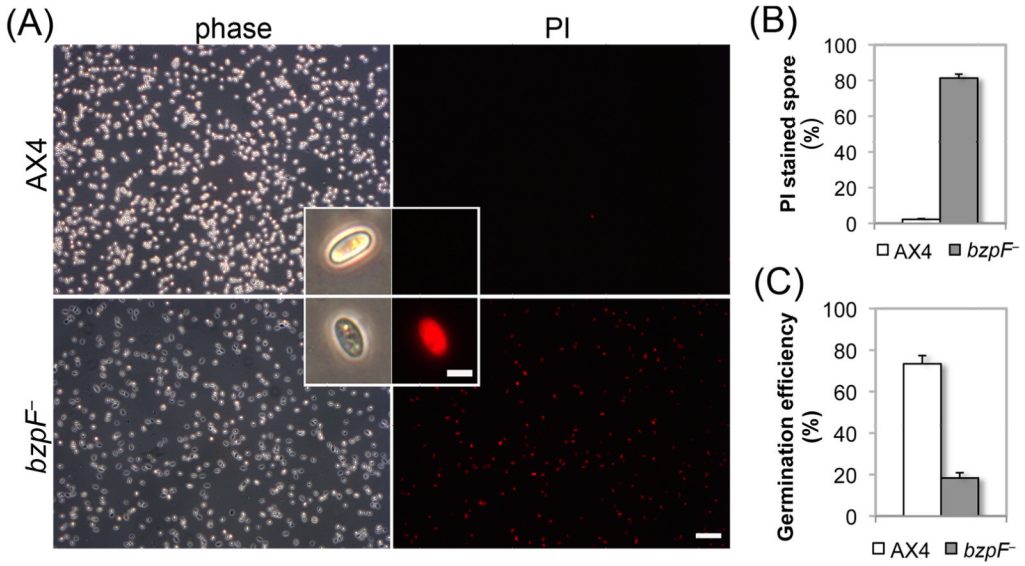

Fig. 4. *bzpF*⁻ spores are compromised

(A) *PI staining of spores*. Phase-contrast (phase) and fluorescence (PI) images of each field of AX4 and *bzpF*⁻ spores, as indicated. Magnified spores are shown as inserts. Bars = 40 μm (low magnification) and 5 μm (inserts). (B) *Quantitation of PI staining:* We counted the PI-stained spores of AX4 (white bar) and *bzpF*⁻ (grey bar) by flow cytometry and the fraction (%) of PI positive-spores is shown (y-axis). Data are the means + s.e.m of five replicates. (C) *Germination:* We incubated AX4 (white bar) and *bzpF*⁻ spores in nutrient medium. The number of germinated amoebae is shown as a fraction (%) of the total spores (y-axis). The data are the means + s.e.m of three replicates.

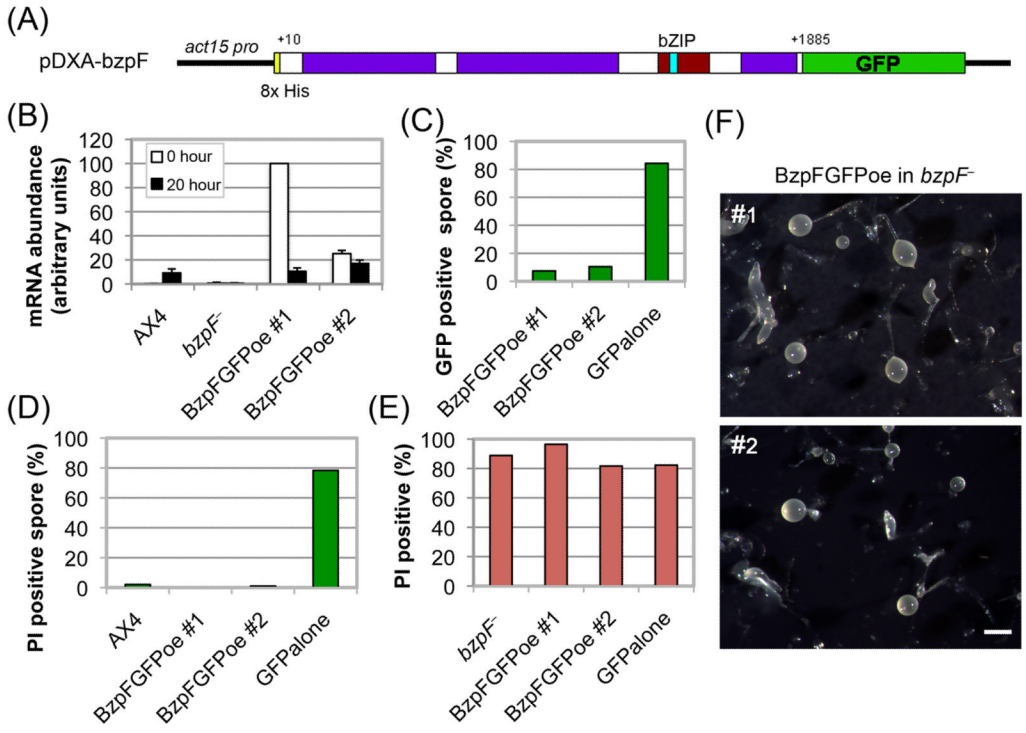

Fig. 5. Ectopic expression of *bzpF* complements the compromised spore phenotype

(A) *The BzpF ectopic expression construct:* We fused most of the *bzpF* coding region (+10 to +1885) with GFP and expressed it in the pDXA vector under the *actin15* promoter in *bzpF*⁻ mutants. (B) *Quantitation of bzpF expression:* We measured the abundance of *bzpF* mRNA in AX4, *bzpF*⁻, and two independent ectopic expression transformants (BzpFGFPoe) by qRT-PCR in vegetative cells (0 hour, white bars) and in developing cells (20 hour, black bars). The data (arbitrary units, y-axis) are the means and standard errors of five replicates. (C) *Partially penetrant expression of BzpF-GFP:* We determined the fraction of GFP positive spores (%, y-axis) by flow cytometry of the ectopic expression strains and of a control strain expressing GFP alone (x-axis). (D) *Complementation of the compromised spore phenotype in spores that express bzpF-GFP*: We stained spores of the indicated strains (x-axis) with PI and used flow cytometry to determine the proportion (%, y-axis) of PI-positive (compromised) spores among the wild type (AX4) and among the GFP-positive spores of the transgenic strains. (E) *Lack of complementation in spores that do not express BzpF-GFP*: We stained spores of the indicated strains (x-axis) with PI and used flow cytometry to determine the proportion (%, y-axis) of PI-positive (compromised) spores among the parental (*bzpF*⁻) and among the GFP-negative spores of the transgenic strains. (F) *The fruiting body morphology of the bzpFoe strains*: Filter development of two *bzpF*-overexpressor strains (#1 and #2) showing morphologies that are nearly identical to the *bzpF*⁻ phenotypes. Bar = 0.5 mm.

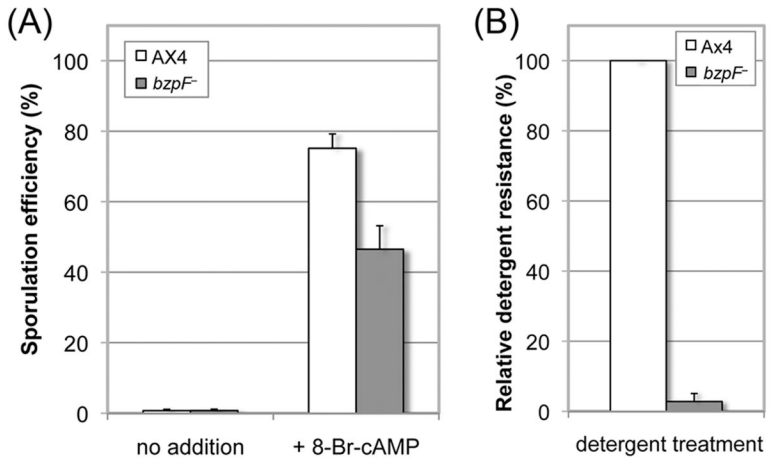

Fig. 6. Activating PKA fails to rescue the sporulation defect of the *bzpF*$^{-}$ mutant

We developed AX4 cells (white bars) and *bzpF*$^{-}$ cells (grey bars), disaggregated them, and incubated them with and without 8-Br-cAMP as indicated. (A) Sporulation efficiency (y-axis) was calculated as the proportion (%) of cells that became spores. The data are the means + s.e.m of 3 replicates. (B) We tested the germination efficiency of 8-Br-cAMP-induced spores by treatment with 0.1% NP-40. The data are presented as the fraction (%) of detergent-resistant spores relative to the total AX4 spores. The data are the means + s.e.m of 4 replicates.

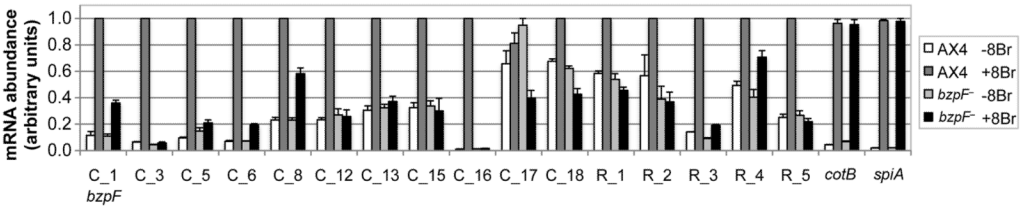

Fig. 7. Candidate BzpF-target genes are regulated by PKA

We developed AX4 and *bzpF*$^{-}$ cells and treated them with or without 8-Br-cAMP as indicated. We then tested the abundance of the candidate target transcripts by quantitative RT-PCR. The gene identities are indicated on the x-axis (Tables S4 and S5). The data are the means + s.e.m of 3-5 replicates, normalized to the maximal abundance of each gene.

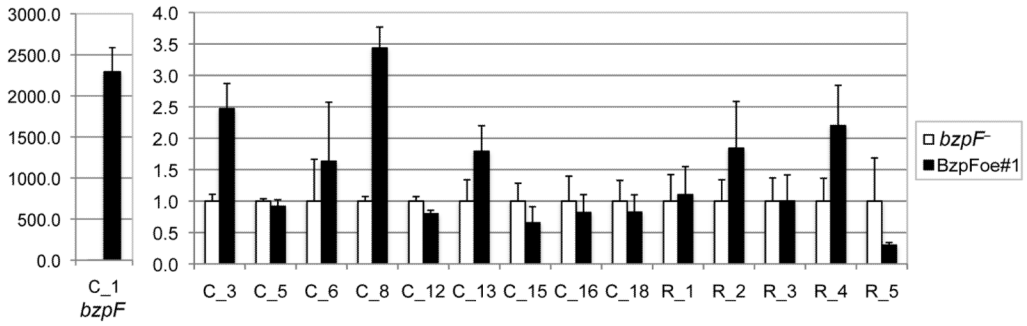

Fig. 8. BzpF is sufficient for expression of its target genes

We used quantitative RT-PCR to test the abundance of putative target transcripts in vegetative *bzpF*– cells (white bars) and *bzpF*-overexpressor cells with the ectopic BzpF-GFP expression vector (black bars). The gene identities are indicated on the x-axis (Tables S4 and S5). The data are the means + s.e.m of 3-9 replicates, normalized to the abundance of each gene in *bzpF*–.

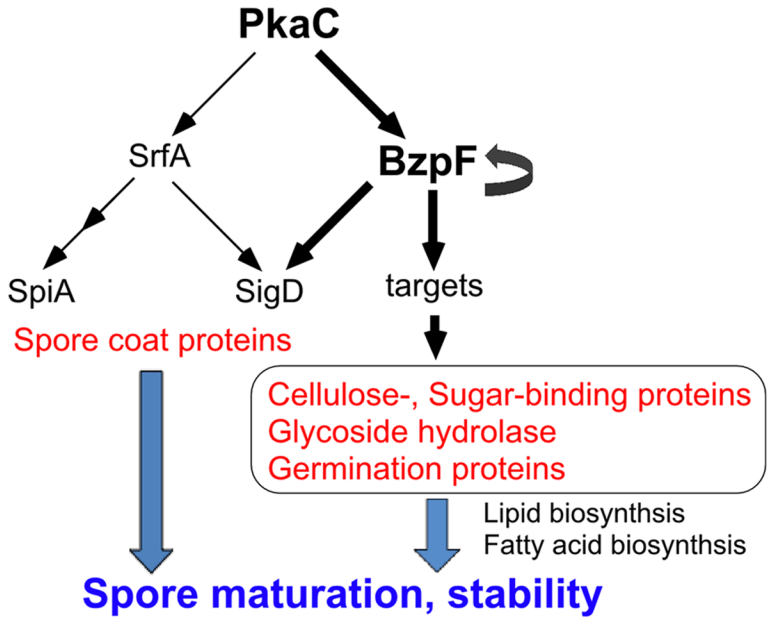

Fig. 9. A proposed model of the PKA-BzpF pathway

PKA regulates several transcription factors including BzpF and SrfA, which are involved in terminal differentiation. Activation of PKA can drive the activation of BzpF, which positively regulates its own expression. BzpF expression is required for spore maturation and stability, probably through direct and indirect transcriptional activation of genes that encode spore coat proteins, cellulose- and sugar-binding proteins, Glycoside hydrolases and germination proteins, as well as lipid and fatty acid biosynthesis.

Dev Biol. Author manuscript; available in PMC 2012 October 1.

Table 1

Gene Ontology analysis of transcripts that are less abundant in *bzpF*$^{-}$

Log_2(AX4/*bzpF*$^{-}$)	matched (%)/input genes	GO term	Category	P-value	Enrichment
>1	107(52.2%)/205	lipid biosynthetic process	Biological process	0.0582	4.54
		fatty acid biosynthetic	Biological process	0.0582	6.70
>3	26(40.6%)/64	cellulose binding	Molecular function	0.0174	30.49
		sugar binding	Molecular function	0.0174	27.58
		extracellular region	Cellular component	0.0066	13.16